



N-(6-Methoxypyridin-2-yl)-1-(pyridin-2-ylmethyl)-1*H*-pyrazole-3-carboxamide: crystal structure and Hirshfeld surface analysis

Vivek C. Ramani,^a Rina D. Shah,^{a‡} Mukesh M. Jotani^b and Edward R. T. Tiekink^{c*}

Received 6 August 2018

Accepted 12 August 2018

Edited by W. T. A. Harrison, University of Aberdeen, Scotland

‡ Additional correspondence author, e-mail: drrdshah@yahoo.co.in.

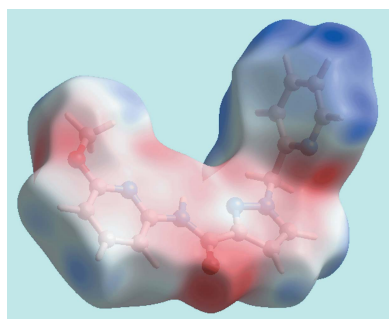
Keywords: crystal structure; pyrazolyl; pyridyl; Hirshfeld surface analysis.**CCDC reference:** 1861657**Supporting information:** this article has supporting information at journals.iucr.org/e

^aDepartment of Chemistry, M. G. Science Institute, Navrangpura, Ahmedabad, Gujarat 38009, India, ^bDepartment of Physics, Bhavan's Sheth R. A. College of Science, Ahmedabad, Gujarat 380 001, India, and ^cResearch Centre for Crystalline Materials, School of Science and Technology, Sunway University, 47500 Bandar Sunway, Selangor Darul Ehsan, Malaysia. *Correspondence e-mail: edwardt@sunway.edu.my

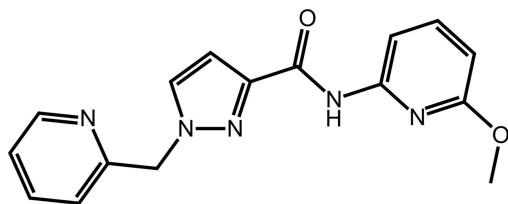
The title compound, C₁₆H₁₅N₅O₂, adopts the shape of the letter *L* with the dihedral angle between the outer pyridyl rings being 78.37 (5)°; the dihedral angles between the central pyrazolyl ring (r.m.s. deviation = 0.0023 Å) and the methylene-bound pyridyl and methoxypyridyl rings are 77.68 (5) and 7.84 (10)°, respectively. Intramolecular amide-N—H···N(pyrazolyl) and pyridyl-C—H···O(amide) interactions are evident and these preclude the participation of the amide-N—H and O atoms in intermolecular interactions. The most notable feature of the molecular packing is the formation of linear supramolecular chains aligned along the *b*-axis direction mediated by weak carbonyl-C=O···π(triazolyl) interactions. An analysis of the calculated Hirshfeld surfaces point to the importance of H···H (46.4%), C···H (22.4%), O···H (11.9%) and N···H (11.1%) contacts in the crystal.

1. Chemical context

Amide bond formation involving acid–amine coupling is an important synthetic tool for the manufacture of pharmaceuticals and fine chemicals (Schuele *et al.*, 2008). The use of a variety of acid–amine coupling agents, most commonly carbodiimides and onium salts such as phosphonium as well as ammonium salts, for amide bond synthesis has been reviewed (Al-Warhi *et al.* 2012; Urich *et al.*, 2014). In this context, *n*-propanephosphonic acid anhydride (T3P) has proved to be an excellent reagent for amide or peptide bond formation. The synthesis of amide bonds utilizing T3P offers high yields, low epimerization and avoids the use of hazardous additives such as explosive hydroxybenzotriazole (HOBt). Further, reactions occur with high yields and lead to the easy removal of the by-products with a simple work-up, overall resulting in the formation of high-quality product. In addition, it is noted that the T3P reagent is non-toxic and non-allergenic (Joullie & Lassen, 2010; Fennie & Roth, 2016). Moreover, amine bond formation between pyrazole and pyrimidine ring systems can lead to the formation of biologically accepted ingredients such as AM251 (Xi *et al.*, 2006), as a CB1 cannabinoid receptor antagonist, and Meclintertant (SR48692; Liu *et al.*, 2017), a neurotensinreceptor (NTS) antagonist. The combination of such moieties can also lead to molecules with anti-tuberculosis, anti-cancer, anti-bacterial and anti-fungal activities (Fustero *et al.*, 2009; Pal *et al.*, 2012; Dar & Shamsuzzaman, 2015; Sapra *et al.*, 2016). As part of our studies in this area, acid–amine coupling between heterocycles such as pyrazole



and pyridine using efficient coupling reagents such as T3P was performed; herein, the crystal and molecular structures of (I) are described along with an analysis of its calculated Hirshfeld surface.



2. Structural commentary

The molecular structure of (I), Fig. 1, comprises an almost planar bi-substituted pyrazolyl ring with the r.m.s. deviation of the fitted atoms being 0.0023 Å. Connected to the ring at the N2 position is a methyl-2-pyridyl residue with the dihedral angle between the five- and six-membered rings being 77.68 (5)°, indicating an almost orthogonal relationship. A substituted amide (C10/N4/O1) group is connected at the C3-position, which is approximately co-planar with the pyrazolyl ring, forming a dihedral angle of 3.5 (3)°. The dihedral angle between the amide atoms and the appended N5-pyridyl ring is 4.4 (3)°, indicating a co-planar relationship. The dihedral angle between the pyridyl rings in (I) of 78.37 (5)° indicates that the molecule has an approximate *L*-shape. The amide-N4—H4N atom is flanked on either side by the pyrazolyl-N1 and pyridyl-N5 atoms and in the same way, the amide-O1 atom accepts a weak intramolecular interaction from the C15—H15 grouping; see Table 1 for geometric data characterizing these interactions. Finally, the methoxy group is approximately co-planar with the pyridyl ring to which it is attached, as seen in the C16—O2—C12—N5 torsion angle of 4.2 (3)°.

3. Supramolecular features

The molecular packing of (I) is largely devoid of structure-directing interactions as the key amide atoms are involved in

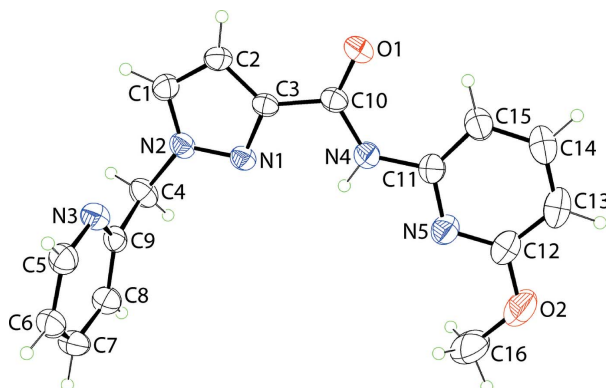


Figure 1
The molecular structure of (I), showing displacement ellipsoids at the 50% probability level.

Table 1

Intra- and intermolecular interactions (Å, °) for (I).

Cg1 is the centroid of the N1/N2/C1—C3 ring.

<i>D</i> —H... <i>A</i>	<i>D</i> —H	H... <i>A</i>	<i>D</i> ... <i>A</i>	<i>D</i> —H... <i>A</i>
N4—H4N...N1	0.86 (1)	2.24 (2)	2.6939 (18)	113 (1)
C15—H15...O1	0.93	2.33	2.909 (2)	120
C10—O1...Cg1 ¹	1.22 (1)	3.42 (1)	3.5486 (16)	86 (1)

Symmetry code: (i) *x*, *y* + 1, *z*.

intramolecular contacts. The only identified directional interaction less than van der Waals separations (Spek, 2009) is a carbonyl-C10=O2... π (triazolyl) contact, Table 1. As illustrated in Fig. 2*a*, these lead to linear supramolecular chains aligned along the *b*-axis direction. The supramolecular chains pack without specific interactions between them, Fig. 2*b*.

4. Hirshfeld surface analysis

The Hirshfeld surfaces calculated for (I) were performed in accord with recent studies (Jotani *et al.*, 2016) and provide additional information on the influence of short interatomic contacts influential in the molecular packing. On the Hirshfeld

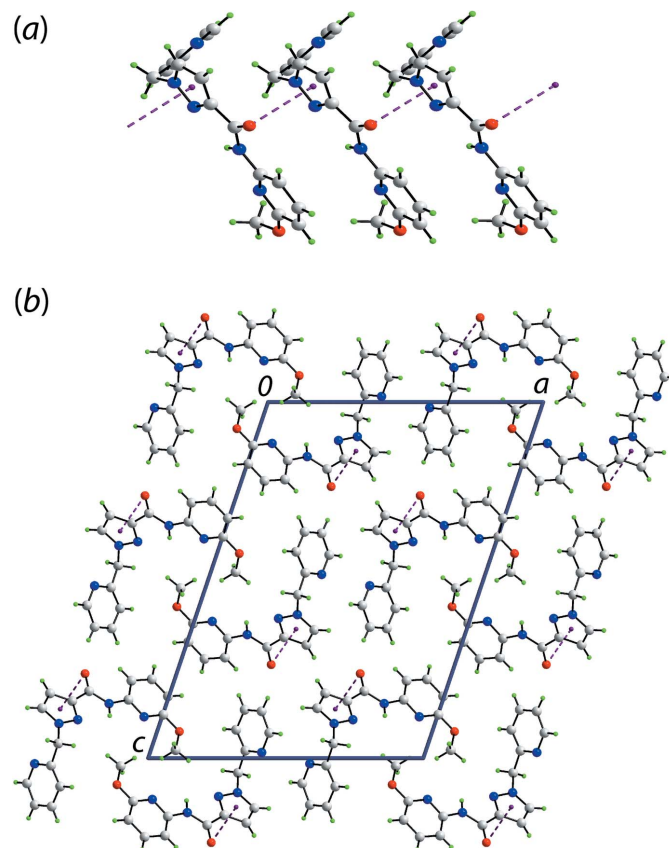


Figure 2
Supramolecular association in the crystal of (I): (a) a view of the supramolecular chain along the *b*-axis direction sustained by carbonyl-C=O... π (triazolyl) interactions shown as purple dashed lines and (b) a view of the unit-cell contents shown in projection down the *b* axis.

Table 3
Percentage contributions of interatomic contacts to the Hirshfeld surface for (I).

Contact	Percentage contribution
H···H	46.4
O···H/H···O	11.9
N···H/H···N	11.1
C···H/H···C	22.4
C···N/N···C	3.5
C···O/O···C	1.9
N···N	1.3
C···C	1.2
N···O/O···N	0.4

Table 2
Summary of short interatomic contacts (Å) in (I).

Contact	Distance	Symmetry operation
O1···H6	2.47	$x, \frac{3}{2} - y, \frac{1}{2} + z$
N1···H16B	2.58	$-x, 1 - y, -z$
N3···H5	2.54	$1 - x, 1 - y, -z$
C6···H1	2.72	$1 - x, -y, z$
C5···C8	3.380 (3)	$x, 1 + y, z$

surfaces mapped over d_{norm} in Fig. 3, the presence of diminutive red spots near the pyrazole-N1, methyl-H16B, pyridyl-N3 and pyridyl-H5 atoms are indicative of short interatomic N···H/H···N contacts (Table 2). In addition, the presence of diminutive red spots near the carbonyl-O1 and pyridyl-H6 atoms on the surface connect the molecules through short interatomic O···H/H···O contacts (Table 2) are highlighted through black dashed lines in Fig. 3a. The faint-red spots appearing near the pyridyl-C5, C6 and C8 atoms and the pyrazolyl-H1 atom in Fig. 3b represent the short interatomic C···C and C···H/H···C contacts (Table 3) between these atoms. The intermolecular C=O··· π contacts connecting the molecules along the *b*-axis direction are illustrated in Fig. 3c. The weak intermolecular interactions described above are also viewed as the blue and red regions near the respective atoms on the Hirshfeld surfaces mapped over the calculated electrostatic potential shown in Fig. 4.

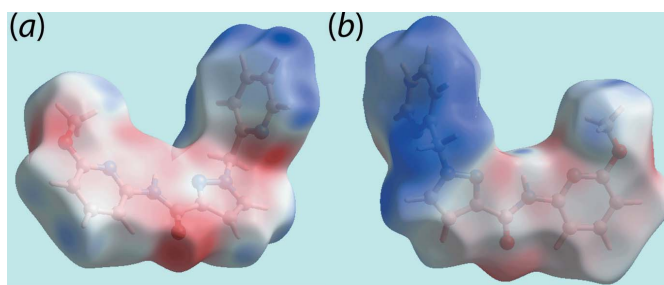


Figure 4
Two views of the Hirshfeld surface mapped over the electrostatic potential in the range -0.080 to $+0.044$ a.u. The red and blue regions represent negative and positive electrostatic potentials, respectively.

The overall two-dimensional fingerprint plot for (I), Fig. 5a, and those delineated into H···H, N···H/H···N, O···H/H···O, C···H/H···C and C···C contacts (McKinnon *et al.*, 2007) are illustrated in Fig. 5b–f, respectively, and the percentage contributions from the different interatomic contacts to the Hirshfeld surface are summarized in Table 3. The greatest, *i.e.* 46.4%, contribution to the Hirshfeld surfaces are from H···H contacts and indicates the significance of dispersive forces on the molecular packing as the interatomic distances involving these contacts are greater than the sum of van der Waals radii. The short interatomic O···H/H···O and C···H/H···C contacts in the crystal structure of (I) are characterized as the pair of thin needle-like and forceps-like tips at $d_e + d_i \sim 2.5$ Å and 2.7 Å, respectively, in the corresponding delineated fingerprint plots Fig. 5c and e. The pair of spikes with the tips at $d_e + d_i \sim 2.6$ Å and the regions of green points aligned in the fingerprint plot delineated into N···H/H···N contacts, Fig. 5d, are indicative of short N···H interatomic contacts (Table 2). In the fingerprint plot delineated into C···C contacts, Fig. 5f, the presence of points at $d_e + d_i < 3.4$ Å, *i.e.* less than the sum of van der Waals radii, are due to short interatomic C5···C8 contacts involving pyridyl-carbon atoms (Fig. 3b) although the contribution from these contacts is relatively small. The notable percentage contributions from O···N/N···O and C···O/O···C contacts to the Hirshfeld

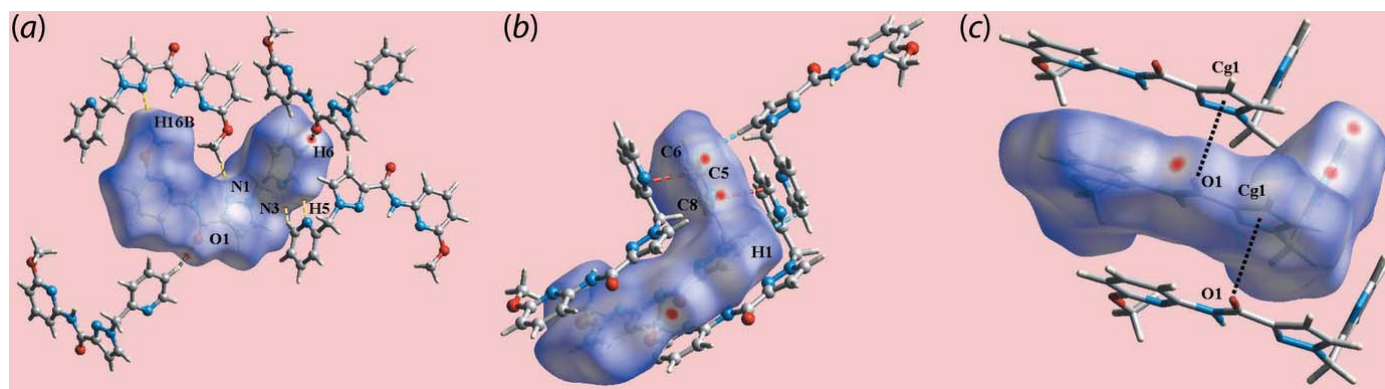


Figure 3
Three views of the Hirshfeld surface for (I) mapped over d_{norm} in the range -0.093 to $+1.418$ a.u. highlighting (a) short interatomic O···H/H···O (yellow dashed lines) and N···H/H···N (black) contacts dashed lines, (b) C···C (red) and C···H/H···C (sky-blue) contacts and (c) C=O··· π contacts (black dotted lines).

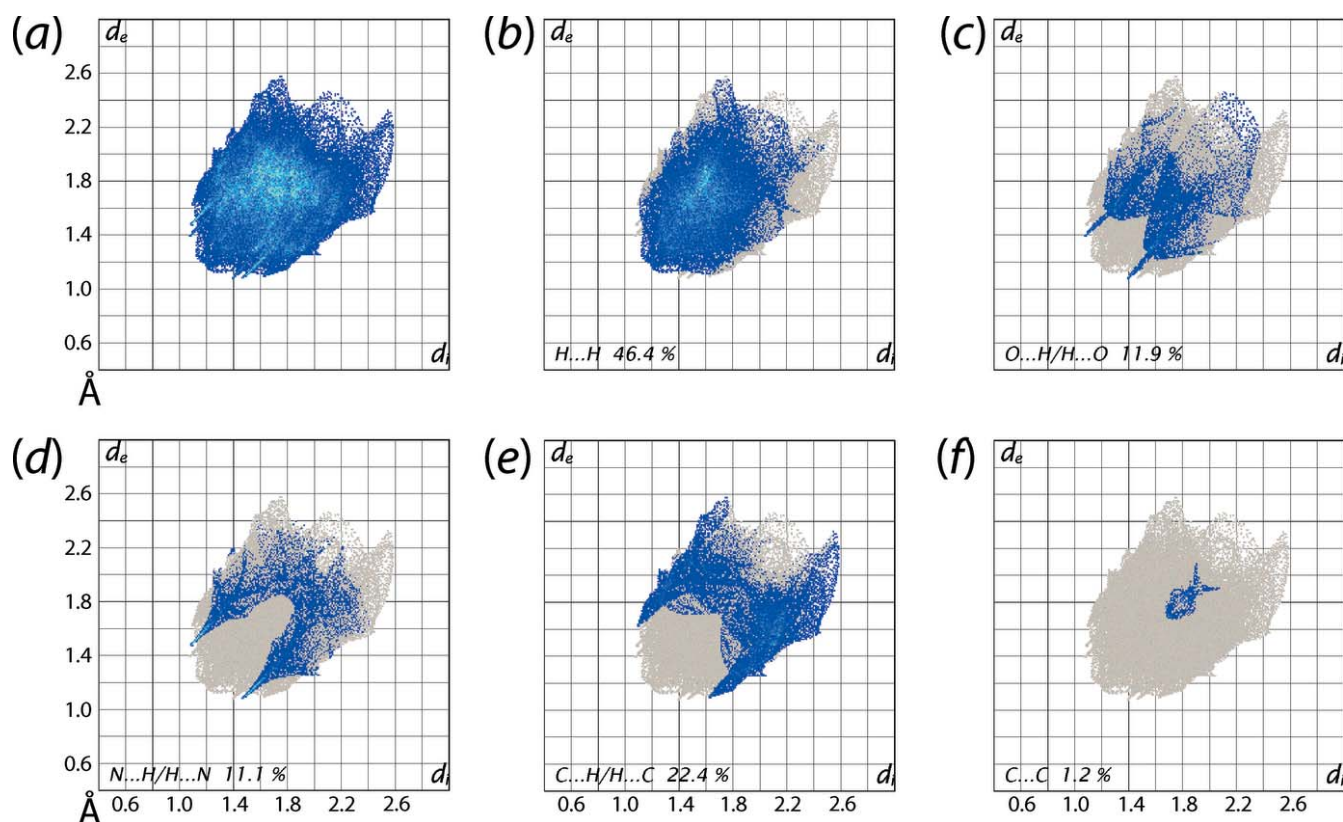


Figure 5

(a) The full two-dimensional fingerprint plot for (I) and (b)–(f) those delineated into H...H, O...H/H...O, N...H/H...N, C...H/H...C and C...C contacts, respectively.

surfaces (Table 2) in the crystal arise from the presence of the intermolecular C=O... π contacts. The interatomic N...N contacts show no significant contribution to the packing of (I).

5. Database survey

The 1,3 N–C and C–C(=O)N(H)–C substitution pattern observed in (I), with hydrogen atoms at the C1 and C2 positions, is unprecedented in structural chemistry according to a search of the Cambridge Structural Database (CSD Version 5.39, May update; Groom *et al.*, 2016). There are considerably more examples of structures with substituents at one of and at both the C1 and C2 positions but none of these are pyridyl groups.

6. Synthesis and crystallization

1*H*-Pyrazole-4-carboxylic acid (0.0446 mol) was treated with diisopropylethyl amine (0.0669 mol) and 1-propane phosphonic acid (T3P) (0.0669 mol) in dimethyl formamide (10 ml) at 273 K for 15 min. Then, 6-methoxypyridin-2-amine (0.0490 mol) was added at 273 K. The reaction mixture was heated at 353 K for 3 h. After completion of the reaction, the product was extracted with ethyl acetate and the excess solvent was removed under vacuum. The product was recrystallized using methanol as solvent to yield 1-(6-methoxypyridin-2-ylmethyl)-1*H*-pyrazole-4-carboxylic acid. This

product (0.0246 mol) and 2-(chloromethyl)pyridine (0.0295 mol) were dissolved in acetone (10 ml), potassium carbonate (0.0369) was added and the reaction mixture was heated at 329 K for 5 h. After completion of the reaction, the product was extracted with ethyl acetate twice (5 ml) and the extract was concentrated under vacuum. The product was washed with diethyl ether (3 ml) and recrystallized from methanol solution to obtain the title compound, (I), as colourless blocks in 88% yield. M.p. 414–415 K. CHN analysis: calculated. C, 62.13; H, 4.89; N, 22.64%; observed: C, 62.06; H, 4.81; N, 22.84%.

7. Refinement details

Crystal data, data collection and structure refinement details are summarized in Table 4. The carbon-bound H atoms were placed in calculated positions (C–H = 0.93–0.97 Å) and were included in the refinement in the riding-model approximation, with $U_{\text{iso}}(\text{H})$ set to 1.2–1.5 $U_{\text{eq}}(\text{C})$. The N-bound H atoms was refined with a distance restraint of 0.86 ± 0.01 Å, and with $U_{\text{iso}}(\text{H}) = 1.2U_{\text{eq}}(\text{N})$.

Acknowledgements

The authors are thankful to the M. G. Science Institute for access to laboratory facilities and to the Centre for Excellence, National Facility for Drug Discovery, Saurashtra University, Rajkot, Gujarat, for the X-ray data collection.

References

Al-Warhi, T. I., Al-Hazimi, H. M. A. & El-Faham, A. (2012). *J. Saudi Chem. Soc.* **16**, 97–116.

Brandenburg, K. (2006). *DIAMOND*. Crystal Impact GbR, Bonn, Germany.

Dar, A. M. & Shamsuzzaman (2015). *J. Nucl. Med. Radiat. Ther.* **6**, art. no. 250 (5 pages). DOI: 10.4172/2155-9619.1000250

Farrugia, L. J. (2012). *J. Appl. Cryst.* **45**, 849–854.

Fennie, M. W. & Roth, J. M. (2016). *J. Chem. Educ.* **93**, 1788–1793.

Fustero, S., Simón-Fuentes, A. & Sanz-Cervera, J. F. (2009). *Org. Prep. Proced. Int.* **41**, 253–290.

Groom, C. R., Bruno, I. J., Lightfoot, M. P. & Ward, S. C. (2016). *Acta Cryst.* **B72**, 171–179.

Jotani, M. M., Wardell, J. L. & Tiekink, E. R. T. (2016). *Z. Kristallogr.* **231**, 247–255.

Joullie, M. M. & Lassen, K. M. (2010). *Arkivoc*, **8**, 189–250.

Liu, J., Agopiantz, M., Poupon, J., Wu, Z., Just, P.-A., Borghese, B., Ségal-Bendirdjian, E., Gauchotte, G., Gompel, A. & Forgez, P. (2017). *Clin. Cancer Res.* **23**, 6516–6528.

McKinnon, J. J., Jayatilaka, D. & Spackman, M. A. (2007). *Chem. Commun.* pp. 3814–3816.

Pal, D., Saha, S. & Singh, S. (2012). *Int. J. Pharm. Pharm. Sci.* **4**, 98–104.

Rigaku (1998). *REQAB*. Rigaku Corporation, Tokyo, Japan.

Rigaku (2011). *CrystalClear-SM Expert*. Rigaku Corporation, Tokyo, Japan.

Sapra, S., Sharma, K., Bhalla, Y. & Dhar, K. L. (2016). *Chem. Sci. J.* **7** art. no. 1000129 (8 pages). DOI: 10.4172/2150-3494.1000129.

Schuele, G., Barnett, S., Bapst, B., Cavaliero, T., Luempert, L., Strehlau, G., Young, D. R., Moran, C. & Junquera, P. (2008). *Vet. Parasitol.* **154**, 311–317.

Sheldrick, G. M. (2008). *Acta Cryst.* **A64**, 112–122.

Sheldrick, G. M. (2015). *Acta Cryst.* **C71**, 3–8.

Spek, A. L. (2009). *Acta Cryst.* **D65**, 148–155.

Urich, R., Grimaldi, R., Luksch, T., Frearson, J. A., Brenk, R. & Wyatt, P. G. (2014). *J. Med. Chem.* **57**, 7536–7549.

Westrip, S. P. (2010). *J. Appl. Cryst.* **43**, 920–925.

Table 4

Experimental details.

Crystal data	
Chemical formula	C ₁₆ H ₁₅ N ₅ O ₂
<i>M_r</i>	309.33
Crystal system, space group	Monoclinic, <i>P</i> ₂ ₁ / <i>c</i>
Temperature (K)	293
<i>a</i> , <i>b</i> , <i>c</i> (Å)	15.8867 (15), 4.6473 (4), 21.6740 (19)
β (°)	108.623 (3)
<i>V</i> (Å ³)	1516.4 (2)
<i>Z</i>	4
Radiation type	Mo <i>K</i> α
μ (mm ⁻¹)	0.09
Crystal size (mm)	0.47 × 0.43 × 0.28
Data collection	
Diffractionmeter	Rigaku SCX mini
Absorption correction	Multi-scan (<i>REQAB</i> ; Rigaku, 1998)
<i>T_{min}</i> , <i>T_{max}</i>	0.808, 0.974
No. of measured, independent and observed [<i>I</i> > 2 σ (<i>I</i>)] reflections	14205, 3458, 2354
<i>R_{int}</i>	0.031
(<i>sin</i> θ / λ) _{max} (Å ⁻¹)	0.649
Refinement	
<i>R</i> [<i>F</i> ² > 2 σ (<i>F</i> ²)], <i>wR</i> (<i>F</i> ²), <i>S</i>	0.042, 0.117, 1.02
No. of reflections	3458
No. of parameters	212
No. of restraints	1
H-atom treatment	H atoms treated by a mixture of independent and constrained refinement
$\Delta\rho_{max}$, $\Delta\rho_{min}$ (e Å ⁻³)	0.13, -0.17

Computer programs: *CrystalClear-SM Expert* (Rigaku, 2011), *SHELXS97* (Sheldrick, 2008), *SHELXL2014* (Sheldrick, 2015), *ORTEP-3 for Windows* (Farrugia, 2012), *DIAMOND* (Brandenburg, 2006) and *pubCIF* (Westrip, 2010).

Xi, Z.-X., Gilbert, J. G., Peng, X. Q., Pak, A. C., Li, X. & Gardner, E. L. (2006). *J. Neurosci.* **26**, 8531–8536.

supporting information

Acta Cryst. (2018). E74, 1254-1258 [https://doi.org/10.1107/S2056989018011477]

N-(6-Methoxypyridin-2-yl)-1-(pyridin-2-ylmethyl)-1*H*-pyrazole-3-carboxamide: crystal structure and Hirshfeld surface analysis

Vivek C. Ramani, Rina D. Shah, Mukesh M. Jotani and Edward R. T. Tiekink

Computing details

Data collection: *CrystalClear-SM Expert* (Rigaku, 2011); cell refinement: *CrystalClear-SM Expert* (Rigaku, 2011); data reduction: *CrystalClear-SM Expert* (Rigaku, 2011); program(s) used to solve structure: *SHELXS97* (Sheldrick, 2008); program(s) used to refine structure: *SHELXL2014* (Sheldrick, 2015); molecular graphics: *ORTEP-3 for Windows* (Farrugia, 2012) and *DIAMOND* (Brandenburg, 2006); software used to prepare material for publication: *publCIF* (Westrip, 2010).

N-(6-Methoxypyridin-2-yl)-1-(pyridin-2-ylmethyl)-1*H*-pyrazole-3-carboxamide

Crystal data

$C_{16}H_{15}N_5O_2$

$M_r = 309.33$

Monoclinic, $P2_1/c$

$a = 15.8867$ (15) Å

$b = 4.6473$ (4) Å

$c = 21.6740$ (19) Å

$\beta = 108.623$ (3)°

$V = 1516.4$ (2) Å³

$Z = 4$

$F(000) = 648$

$D_x = 1.355$ Mg m⁻³

Mo $K\alpha$ radiation, $\lambda = 0.71073$ Å

Cell parameters from 11059 reflections

$\theta = 3.2\text{--}27.7^\circ$

$\mu = 0.09$ mm⁻¹

$T = 293$ K

Block, colourless

$0.47 \times 0.43 \times 0.28$ mm

Data collection

Rigaku SCX mini

diffractometer

Detector resolution: 6.849 pixels mm⁻¹

ω scans

Absorption correction: multi-scan

(*REQAB*; Rigaku, 1998)

$T_{\min} = 0.808$, $T_{\max} = 0.974$

14205 measured reflections

3458 independent reflections

2354 reflections with $I > 2\sigma(I)$

$R_{\text{int}} = 0.031$

$\theta_{\max} = 27.5^\circ$, $\theta_{\min} = 3.8^\circ$

$h = -19 \rightarrow 20$

$k = -6 \rightarrow 6$

$l = -28 \rightarrow 28$

Refinement

Refinement on F^2

Least-squares matrix: full

$R[F^2 > 2\sigma(F^2)] = 0.042$

$wR(F^2) = 0.117$

$S = 1.02$

3458 reflections

212 parameters

1 restraint

Hydrogen site location: mixed

H atoms treated by a mixture of independent

and constrained refinement

$w = 1/[\sigma^2(F_o^2) + (0.0534P)^2 + 0.1998P]$

where $P = (F_o^2 + 2F_c^2)/3$

$(\Delta/\sigma)_{\max} < 0.001$

$\Delta\rho_{\max} = 0.13$ e Å⁻³

$\Delta\rho_{\min} = -0.17$ e Å⁻³

Special details

Geometry. All esds (except the esd in the dihedral angle between two l.s. planes) are estimated using the full covariance matrix. The cell esds are taken into account individually in the estimation of esds in distances, angles and torsion angles; correlations between esds in cell parameters are only used when they are defined by crystal symmetry. An approximate (isotropic) treatment of cell esds is used for estimating esds involving l.s. planes.

Fractional atomic coordinates and isotropic or equivalent isotropic displacement parameters (\AA^2)

	<i>x</i>	<i>y</i>	<i>z</i>	$U_{\text{iso}}^*/U_{\text{eq}}$
O1	0.33267 (7)	0.7478 (2)	0.23734 (5)	0.0605 (3)
O2	-0.08095 (9)	0.9148 (4)	0.07466 (8)	0.1027 (5)
N1	0.30289 (8)	0.2514 (2)	0.10788 (5)	0.0434 (3)
N2	0.36665 (8)	0.0898 (2)	0.09706 (5)	0.0457 (3)
N3	0.40561 (8)	0.2467 (3)	-0.01587 (6)	0.0511 (3)
N4	0.20890 (8)	0.6321 (3)	0.15313 (6)	0.0516 (3)
H4N	0.1920 (10)	0.521 (3)	0.1198 (6)	0.062*
N5	0.06549 (9)	0.7801 (3)	0.11608 (7)	0.0577 (4)
C1	0.44689 (10)	0.1427 (3)	0.14031 (7)	0.0517 (4)
H1	0.5001	0.0558	0.1415	0.062*
C2	0.43609 (10)	0.3459 (3)	0.18194 (7)	0.0483 (4)
H2	0.4795	0.4266	0.2172	0.058*
C3	0.34578 (9)	0.4073 (3)	0.16025 (6)	0.0408 (3)
C4	0.34470 (12)	-0.1001 (3)	0.04122 (7)	0.0548 (4)
H4A	0.2866	-0.1833	0.0350	0.066*
H4B	0.3874	-0.2563	0.0502	0.066*
C5	0.34405 (10)	0.0471 (3)	-0.02091 (6)	0.0438 (3)
C6	0.40938 (11)	0.3653 (4)	-0.07088 (7)	0.0567 (4)
H6	0.4516	0.5076	-0.0679	0.068*
C7	0.35489 (12)	0.2904 (4)	-0.13146 (8)	0.0615 (5)
H7	0.3609	0.3760	-0.1686	0.074*
C8	0.29151 (12)	0.0865 (4)	-0.13579 (8)	0.0663 (5)
H8	0.2530	0.0310	-0.1762	0.080*
C9	0.28514 (11)	-0.0364 (4)	-0.07958 (7)	0.0573 (4)
H9	0.2417	-0.1733	-0.0814	0.069*
C10	0.29654 (9)	0.6120 (3)	0.18811 (6)	0.0442 (3)
C11	0.14308 (10)	0.8033 (3)	0.16395 (7)	0.0488 (4)
C12	-0.00155 (11)	0.9321 (4)	0.12181 (9)	0.0682 (5)
C13	0.00381 (13)	1.1138 (4)	0.17359 (11)	0.0755 (5)
H13	-0.0451	1.2186	0.1755	0.091*
C14	0.08339 (13)	1.1327 (4)	0.22134 (10)	0.0722 (5)
H14	0.0895	1.2520	0.2570	0.087*
C15	0.15550 (12)	0.9762 (4)	0.21746 (8)	0.0611 (4)
H15	0.2104	0.9875	0.2499	0.073*
C16	-0.08995 (15)	0.7152 (6)	0.02254 (13)	0.1148 (9)
H16A	-0.0495	0.7665	-0.0005	0.172*
H16B	-0.1497	0.7207	-0.0068	0.172*
H16C	-0.0766	0.5245	0.0400	0.172*

Atomic displacement parameters (Å²)

	U^{11}	U^{22}	U^{33}	U^{12}	U^{13}	U^{23}
O1	0.0609 (7)	0.0742 (7)	0.0434 (6)	−0.0007 (6)	0.0123 (5)	−0.0163 (5)
O2	0.0550 (8)	0.1215 (13)	0.1194 (12)	0.0237 (8)	0.0108 (8)	−0.0180 (11)
N1	0.0491 (7)	0.0441 (6)	0.0367 (6)	0.0006 (5)	0.0130 (5)	0.0019 (5)
N2	0.0561 (7)	0.0435 (6)	0.0385 (6)	0.0048 (6)	0.0166 (5)	0.0020 (5)
N3	0.0564 (8)	0.0524 (7)	0.0433 (7)	0.0002 (6)	0.0142 (6)	0.0009 (6)
N4	0.0473 (7)	0.0551 (8)	0.0505 (7)	0.0009 (6)	0.0129 (6)	−0.0120 (6)
N5	0.0477 (7)	0.0609 (8)	0.0643 (8)	0.0031 (6)	0.0175 (6)	−0.0004 (7)
C1	0.0482 (8)	0.0594 (9)	0.0465 (8)	0.0102 (7)	0.0139 (7)	0.0080 (7)
C2	0.0463 (8)	0.0567 (9)	0.0374 (7)	0.0026 (7)	0.0073 (6)	0.0039 (7)
C3	0.0462 (8)	0.0439 (7)	0.0312 (6)	−0.0011 (6)	0.0109 (6)	0.0050 (6)
C4	0.0765 (11)	0.0416 (8)	0.0490 (8)	0.0004 (8)	0.0240 (8)	−0.0025 (7)
C5	0.0505 (8)	0.0399 (7)	0.0428 (7)	0.0091 (6)	0.0175 (6)	−0.0028 (6)
C6	0.0583 (9)	0.0605 (10)	0.0550 (9)	0.0030 (8)	0.0235 (8)	0.0070 (8)
C7	0.0692 (11)	0.0741 (11)	0.0438 (8)	0.0168 (9)	0.0215 (8)	0.0106 (8)
C8	0.0682 (11)	0.0806 (12)	0.0412 (8)	0.0107 (10)	0.0050 (8)	−0.0063 (8)
C9	0.0570 (9)	0.0597 (10)	0.0525 (9)	−0.0012 (8)	0.0138 (7)	−0.0064 (8)
C10	0.0492 (8)	0.0478 (8)	0.0360 (7)	−0.0035 (7)	0.0141 (6)	0.0024 (6)
C11	0.0493 (8)	0.0467 (8)	0.0545 (9)	−0.0021 (7)	0.0222 (7)	0.0018 (7)
C12	0.0516 (10)	0.0708 (11)	0.0842 (13)	0.0081 (9)	0.0245 (9)	0.0051 (10)
C13	0.0673 (12)	0.0695 (12)	0.1041 (15)	0.0109 (10)	0.0478 (12)	0.0003 (11)
C14	0.0789 (13)	0.0668 (11)	0.0847 (13)	−0.0001 (10)	0.0455 (11)	−0.0141 (10)
C15	0.0621 (10)	0.0615 (10)	0.0648 (10)	−0.0035 (8)	0.0274 (8)	−0.0103 (8)
C16	0.0657 (13)	0.134 (2)	0.1161 (19)	0.0129 (14)	−0.0116 (13)	−0.0294 (18)

Geometric parameters (Å, °)

O1—C10	1.2147 (16)	C4—H4A	0.9700
O2—C12	1.349 (2)	C4—H4B	0.9700
O2—C16	1.433 (3)	C5—C9	1.372 (2)
N1—C3	1.3354 (17)	C6—C7	1.367 (2)
N1—N2	1.3404 (16)	C6—H6	0.9300
N2—C1	1.3421 (18)	C7—C8	1.364 (3)
N2—C4	1.4476 (18)	C7—H7	0.9300
N3—C5	1.3271 (18)	C8—C9	1.378 (2)
N3—C6	1.3321 (19)	C8—H8	0.9300
N4—C10	1.3593 (18)	C9—H9	0.9300
N4—C11	1.3920 (19)	C11—C15	1.372 (2)
N4—H4N	0.859 (9)	C12—C13	1.385 (3)
N5—C12	1.317 (2)	C13—C14	1.357 (3)
N5—C11	1.338 (2)	C13—H13	0.9300
C1—C2	1.355 (2)	C14—C15	1.382 (2)
C1—H1	0.9300	C14—H14	0.9300
C2—C3	1.3893 (19)	C15—H15	0.9300
C2—H2	0.9300	C16—H16A	0.9600
C3—C10	1.477 (2)	C16—H16B	0.9600

C4—C5	1.508 (2)	C16—H16C	0.9600
C12—O2—C16	118.00 (16)	C8—C7—H7	121.0
C3—N1—N2	104.11 (11)	C6—C7—H7	121.0
N1—N2—C1	112.18 (12)	C7—C8—C9	119.21 (15)
N1—N2—C4	119.62 (12)	C7—C8—H8	120.4
C1—N2—C4	128.10 (13)	C9—C8—H8	120.4
C5—N3—C6	117.26 (13)	C5—C9—C8	118.76 (16)
C10—N4—C11	129.51 (13)	C5—C9—H9	120.6
C10—N4—H4N	114.6 (11)	C8—C9—H9	120.6
C11—N4—H4N	115.8 (11)	O1—C10—N4	124.52 (14)
C12—N5—C11	117.15 (15)	O1—C10—C3	122.02 (13)
N2—C1—C2	107.38 (13)	N4—C10—C3	113.46 (12)
N2—C1—H1	126.3	N5—C11—C15	123.41 (15)
C2—C1—H1	126.3	N5—C11—N4	112.27 (13)
C1—C2—C3	104.75 (13)	C15—C11—N4	124.32 (15)
C1—C2—H2	127.6	N5—C12—O2	119.06 (18)
C3—C2—H2	127.6	N5—C12—C13	124.14 (17)
N1—C3—C2	111.57 (13)	O2—C12—C13	116.80 (17)
N1—C3—C10	120.24 (12)	C14—C13—C12	117.31 (17)
C2—C3—C10	128.18 (13)	C14—C13—H13	121.3
N2—C4—C5	113.65 (12)	C12—C13—H13	121.3
N2—C4—H4A	108.8	C13—C14—C15	120.52 (17)
C5—C4—H4A	108.8	C13—C14—H14	119.7
N2—C4—H4B	108.8	C15—C14—H14	119.7
C5—C4—H4B	108.8	C11—C15—C14	117.47 (17)
H4A—C4—H4B	107.7	C11—C15—H15	121.3
N3—C5—C9	122.73 (14)	C14—C15—H15	121.3
N3—C5—C4	116.68 (13)	O2—C16—H16A	109.5
C9—C5—C4	120.50 (14)	O2—C16—H16B	109.5
N3—C6—C7	123.98 (16)	H16A—C16—H16B	109.5
N3—C6—H6	118.0	O2—C16—H16C	109.5
C7—C6—H6	118.0	H16A—C16—H16C	109.5
C8—C7—C6	118.04 (15)	H16B—C16—H16C	109.5
C3—N1—N2—C1	-0.62 (14)	C11—N4—C10—O1	0.4 (2)
C3—N1—N2—C4	-177.19 (11)	C11—N4—C10—C3	-179.08 (14)
N1—N2—C1—C2	0.51 (16)	N1—C3—C10—O1	176.69 (13)
C4—N2—C1—C2	176.71 (13)	C2—C3—C10—O1	-2.7 (2)
N2—C1—C2—C3	-0.17 (16)	N1—C3—C10—N4	-3.79 (18)
N2—N1—C3—C2	0.50 (14)	C2—C3—C10—N4	176.79 (14)
N2—N1—C3—C10	-179.01 (11)	C12—N5—C11—C15	-0.3 (2)
C1—C2—C3—N1	-0.21 (16)	C12—N5—C11—N4	179.54 (14)
C1—C2—C3—C10	179.25 (13)	C10—N4—C11—N5	175.29 (14)
N1—N2—C4—C5	83.78 (16)	C10—N4—C11—C15	-4.9 (3)
C1—N2—C4—C5	-92.17 (18)	C11—N5—C12—O2	-179.95 (16)
C6—N3—C5—C9	-0.7 (2)	C11—N5—C12—C13	0.5 (3)
C6—N3—C5—C4	175.81 (13)	C16—O2—C12—N5	4.2 (3)

N2—C4—C5—N3	37.45 (19)	C16—O2—C12—C13	-176.20 (19)
N2—C4—C5—C9	-145.99 (14)	N5—C12—C13—C14	-0.5 (3)
C5—N3—C6—C7	-1.0 (2)	O2—C12—C13—C14	179.96 (18)
N3—C6—C7—C8	1.5 (3)	C12—C13—C14—C15	0.2 (3)
C6—C7—C8—C9	-0.4 (3)	N5—C11—C15—C14	0.1 (2)
N3—C5—C9—C8	1.7 (2)	N4—C11—C15—C14	-179.76 (15)
C4—C5—C9—C8	-174.61 (14)	C13—C14—C15—C11	0.0 (3)
C7—C8—C9—C5	-1.2 (2)		

Hydrogen-bond geometry (Å, °)

Cg1 is the centroid of the N1/N2/C1—C3 ring.

<i>D</i> —H... <i>A</i>	<i>D</i> —H	H... <i>A</i>	<i>D</i> ... <i>A</i>	<i>D</i> —H... <i>A</i>
N4—H4 <i>N</i> ...N1	0.86 (1)	2.24 (2)	2.6939 (18)	113 (1)
C15—H15...O1	0.93	2.33	2.909 (2)	120
C10—O1...Cg1 ⁱ	1.22 (1)	3.42 (1)	3.5486 (16)	86 (1)

Symmetry code: (i) *x*, *y*+1, *z*.